CFD Letters

Cattaneo-Christov Heat and Mass Transfer Flux Across Electro-Hydrodynamics Blood-Based Hybrid NanoFluid Subject to Lorentz Force

K.Sandhya Rani[1], G.Venkata Ramana Reddy[2,*]

[1] Research scholar , Department of Engineering Mathematics, Koneru Lakshmaiah Education Foundation, Vaddeswaram, 522302 india
[2] Department of Engineering Mathematics ,Koneru Lakshmaiah Education Foundation ,Vaddeswaram, 522302 india

ARTICLE INFO	ABSTRACT
	This study is unique in that it considers both the magnetic field and the electromagnetic force in the flow direction. The imposed magnetic field causes the fluid flow to slow down, whereas the electric force factor increases the fluid velocity and temperature.The principle aim of the present study is addressing electro-hydrodynamic blood-based hybrid nanofluid behaviour when it passes through a vertical stretchable areas.The theories of the Cattaneo-Christov model were investigated with thermal radiation possessing heat generation in this study. Partial differential equations were used to solve the problem. To look into systems of coupled nonlinear differential equations, the set of equations was simplified using appropriate variables. The answer to simplified equations is obtained using a novel numerical method known as the Spectral relaxation method (SRM). Because it can decouple and linearize the set of equations, the SRM is preferred. The SRM uses the Gauss-Seidel approach as itsfoundation. The analysis of equations were done numerically utilizing spectral relaxation techniques. The outcomes are (i) Higher electric field factor is noticed to enhance both velocity and temperature profile; (ii) Increase in Eckert number is observed to increase both thermal and hydrodynamic boundary layer thickness; (iii) A higher value of K extends the hole and allows for higher fluid flow by increasing the fluid velocity; (iv) Increase in Pr depreciates both velocity and temperature profile; and (v) A higher value of Sc depreciates the skin friction and Sherwood number

1. Introduction

Many people are interested in nanotechnology at the moment. It can be used in a variety of medical fields, including biofluid mechanics. Biological sensors and pharmacological uses. The importance of nanofluids is due to the fact that it is extremely strong and composed of nano-sized particles. Oscillators, optical pairs, optical switches, and tunable optical fiber filters all use magnetic nanofluids. In a cylindrical disk, Waqas *et al.,* [1] investigated magnetized Walter's-B nanofluid. A study by Xia *et al.,* looked into nonlinear mixed convectively hybrid nanofluid fluid flow with an eye toward heat and mass transfer [2]. Nanofluid and dusty particles were studied by Shaheen *et al.,* [3] for the Soret-Dufour mechanism. Couple stress hybrid nanofluid free stream with thermal effect was

studied by Zubair *et al.,* [4]. Sadiq *et al.,* [5] examined the Maxwell nanofluid flow analysis of an Ethylene Glycol/water mixture. Shan *et al.,* [16] utilized an effective thermal conductivity to study magnetite micropolar Casson ferrofluid. When the nanofluid passed a sheet with heat plus mass flux constraints, the results were studied by Mamatha *et al.,* [6].

MHD squeezed progression of Casson dissipative with chemical plus radiative reactions was studied by Akolade *et al.,* [7]. MHD nanoscience and technology, which involves the transfer of heat and mass, is receiving more and more attention. In order to control the flow of electrically conducting fluids, MHD is a device that can be used in both channels and flat plates. Thermal, hydrodynamic and concentration layers establied the moment a fluid is set into motion. The thermal process of MHD is applicable in metallurgy, geophysics, power engineering, MHD accelerators, plasma devices and so on. As a result of the numerous usefulness of MHD nanoscience, many researchers have studied it.

Recent years have seen a surge in interest in using a magnetic field to address heat plus mass phenomena. An MHD Casson flow within an upright penetrable plate with Soret-Dufour mechanisms was studied by Vijaya and Reddy [8]. MHD flow within a permeable porous medium was researched by Suneetha *et al.,* [9] using heat source and radiation reaction. Micropolar fluid moving past a linearly stretchable region was studied by Reddy and Krishna [10] for Soret-Dufour mechanisms in an electrically conducting MHD micropolar system. Nanofluid moving in a stretchable region with a non-constant heat source and variable viscosity was studied by Nagasantoshi *et al.,* [11]. Lakshmi *et al.,* [12] performed a numerical study of MHD flow past a moveable upright penetrable plate with heat and mass transport.

In literature, a large number of authors have taken into account magnetic fields, heat plus mass transport within a permeable stretchable regime. MHD accelerators, power engineering, underground repository systems and geothermal extraction, and polymer additives are just some of the applications that benefit from magnetic fields. Stability point flow and second order slip with radiative effects were explained by Mabood and colleagues [13] because of their numerous applications. Hayat *et al.,* [14] researched the reaction of a rotating disk on radiative flow. Rashidi *et al.,* [16] studied Casson movement in squeezing configuration and thermophysical reaction. In a radiative flow of ferromagnetic Maxwell fluid. Nayak *et al.,* [15] addressed flow of magnetized nano fluids between double parallel pores surfaces.

Hybrid nanofluid flow transport in response to thermal radiation, Joule heating, and viscous dissipative effects is addressed in this paper because of its importance in medicine and biomedical engineering. The blood-based hybrid nanoparticles are studied in terms of magnetic and electromagnetic fields. Thermal and mass flux are taken into account when performing a chemical reaction of the first order. An area that Saeed *et al.,* [17] had overlooked was addressed in the current study. No previous research has examined this model type, as far as we can tell. Due to these applications in power engineering, aerodynamics, engineering, agriculture and others, the current study has great potential.

2. Methodology

Consider an incompressible, steady, laminar flow of electro-hydrodynamic blood-based hybrid nanofluid past a stretching surface. Lorentz force and electric current provide a combine efforts to the flow regime. At the wall, the concentration alongside temperature distribution are denoted by C_w and T_w. Also, C_∞ and T_∞ denoted the free stream concentration and temperature. Within the boundary layer, $C_w < C_\infty$ while $T_w < T_\infty$ which shows a cooled plate. The Joule heating and dissipative reactions are taken to be of great significant. A chemical reaction of first order and thermal

radiation are considered. The physical interpretation are depicted in Figure 1. Based on the boundary layer approximation, the governing equations are:
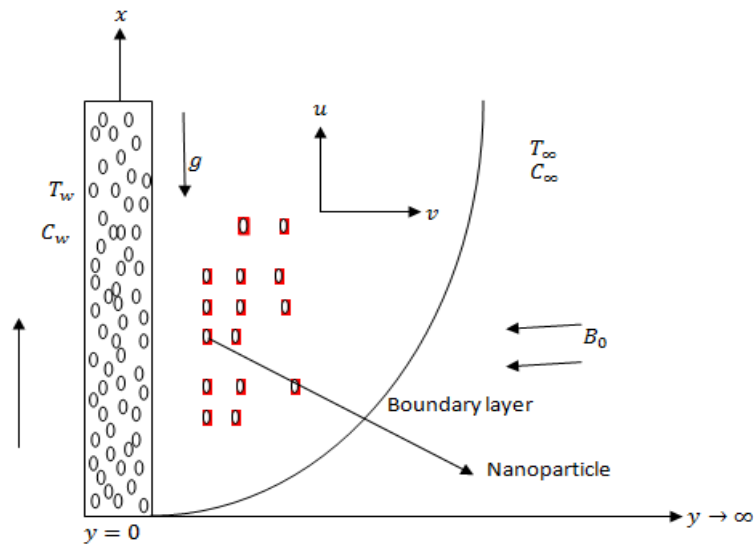

Fig. 1. Physical configuration

$$\frac{\partial u}{\partial x} + \frac{\partial v}{\partial y} = 0 \tag{1}$$

$$u\frac{\partial u}{\partial x} + v\frac{\partial u}{\partial y} = \nu_{hf}\frac{\partial^2 u}{\partial y^2} + \frac{\sigma_{hnf}}{\rho_{hnf}}(E_0 B_0 - B_0^2 u) - \frac{\eta_0}{\rho_{hnf}}\frac{\partial^3 u}{\partial y^3} - \frac{\nu}{K}u \tag{2}$$

$$u\frac{\partial T}{\partial x} + v\frac{\partial T}{\partial y} = \alpha_{hnf}\frac{\partial^2 T}{\partial y^2} + \frac{\mu_{nf}}{(\rho c_p)_{hnf}}\left(\frac{\partial u}{\partial y}\right)^2 + \frac{\sigma_{hnf}}{(\rho c_p)_{hnf}} + \frac{Q_0}{(\rho c_p)_{hnf}}(T - T_\infty) + \tau\left[D_B\frac{\partial C}{\partial y}\frac{\partial T}{\partial y} + \frac{D_T}{T_\infty}\left(\frac{\partial T}{\partial y}\right)^2\right] -$$
$$\beta_1\left[u\frac{\partial u}{\partial x}\frac{\partial T}{\partial x} + v\frac{\partial v}{\partial y}\frac{\partial T}{\partial y} + u\frac{\partial v}{\partial x}\frac{\partial T}{\partial y} + v\frac{\partial u}{\partial y}\frac{\partial T}{\partial x} + 2uv\frac{\partial^2 u}{\partial x\partial y} + u^2\frac{\partial^T}{\partial x^2} + v^2\frac{\partial^2 T}{\partial y^2}\right] \tag{3}$$

$$u\frac{\partial C}{\partial x} + v\frac{\partial C}{\partial y} = D_B\frac{\partial^2 C}{\partial y^2} - k_l(C - C_\infty) - \beta_2\left[u\frac{\partial u}{\partial x}\frac{\partial C}{\partial x} + v\frac{\partial v}{\partial y}\frac{\partial C}{\partial y} + u\frac{\partial v}{\partial x}\frac{\partial C}{\partial y} + v\frac{\partial u}{\partial y}\frac{\partial C}{\partial x} + 2uv\frac{\partial^2 u}{\partial x\partial y} + \right.$$
$$\left. u^2\frac{\partial C}{\partial x^2} + v^2\frac{\partial^2 C}{\partial y^2}\right] \tag{4}$$

the associated boundary conditions are:

$$u = bx = u_w(x), \qquad v = 0, \qquad T = T_w, \qquad C = C_w, \quad at \quad y = 0$$
$$u = v = 0, \; T \longrightarrow T_\infty, \; C \longrightarrow C_\infty, \quad as \quad y \longrightarrow \infty \tag{5}$$

where ρ_{hnf} means hybrid nanofluid density, u, v are velocities component acting along x and y axis, ν_{hnf} means hybrid nanofluid viscosity, σ_{hnf} means hybrid nanofluid electrical conductivity, E_0 means strength of electric field, B_0 means magnetic field strength, α_{hnf} means thermal diffusivity, $(\rho c_p)_{hnf}$ means specific heat capacity, Q_0 means heat absorption/emission, T means fluid temperature, T_∞ means free stream temperature, C means fluid concentration, C_∞ means free stream concentration, T_w and C_w are wall temperature and concentration respectively, u and v means velocity component

in x and y area, η_0 means couple stress coefficient, K means porosity coefficient, c_p means specific heat, τ means Brownian motion coefficient, D_B means mass diffusivity, β_i, β_j are thermal and mass relaxation coefficient, β_1, β_2 are thermal and mass relaxation parameters, k_l means chemical reaction coefficient, b is the stretching constant.

The following suitable similarity transformation are defined in order to simplify the current model

$$\eta = y\sqrt{\frac{b}{v}}, \ \theta(\eta) = \frac{T-T_\infty}{T_w-T_\infty}, \ \phi(\eta) = \frac{C-C_\infty}{C_w-C_\infty}, \ u = bxf'(\eta), \ v = -\sqrt{bv}f(\eta) \tag{6}$$

Using Eq. (6) on Eqs. (1)-(4) subject to (5) to obtain:

$$f''' + \frac{\mu_f \rho_{hnf}}{\mu_{hnf}\rho_f}\left[ff'' - f'^2 - Kf^v + M(E-f') + \frac{1}{Po}f\right] = 0 \tag{7}$$

$$\frac{K_{hnf}}{k_f}\theta'' + Pr\frac{(\rho c_p)_{hnf}}{(\rho c_p)_f}f\theta' + EcPr\left[M(E-f')^2 + \frac{\mu_{hnf}}{\mu_f}(f'')^2\right] + QPr\theta + Nb\phi'\theta' + Nt(\theta')^2 - \beta_1(ff'\theta' + f^2\theta'') = 0 \tag{8}$$

$$\phi'' + Scf\phi' - Cr\phi + \frac{Nt}{LnNb}\theta'' - \beta_2(ff'\phi' + f^2\phi'') = 0 \tag{9}$$

With the constraints:

$$f(0) = 0, \ f'(0) = 1, \ \theta(0) = \phi(0) = 1, f(\infty) = 0, \ \theta(\infty) = \phi(\infty) = 0 \tag{10}$$

The thermo-physical properties for the hybrid nanofluids are defined as follow:

$$\frac{k_{hf}}{k_f} = \frac{2\phi_1\frac{k_{MWCNT}}{(k_{MWCNT}-k_{hf})} - \phi_1 + 1 - In\frac{k_{MWCNT}+k_{hf}}{2k_{hf}}}{2\phi_1\frac{k_{hf}}{(k_{MWCNT}-k_{hf})} - \phi_1 + 1 - In\frac{k_{MWCNT}+k_{hf}}{2k_{hf}}}$$

$$\frac{k_{hnf}}{k_{hf}} = \frac{2\phi_2\frac{k_{SWCNT}}{(k_{MWCNT}-k_{hf})} - \phi_2 + 1 - In\frac{k_{SWCNT}+k_{hf}}{2k_{hf}}}{2\phi_2\frac{k_{hf}}{(k_{SWCNT}-k_{hf})} - \phi_2 + 1 - In\frac{k_{SWCNT}+k_{hf}}{2k_{hf}}}$$

$$\frac{(\rho c_p)_{hnf}}{(\rho c_p)_f} = \left[(1-\phi_2)\left(1 - \left(1 - \frac{(\rho c_p)_{SWCNT}}{(\rho c_p)_f}\right)\phi_1 + \phi_2\frac{(\rho c_p)_{MWCNT}}{(\rho c_p)_f}\right)\right]$$

$$\frac{(\rho_{hnf})}{(\rho_f)} = \left[(1-\phi_2)\left(1 - \left(1 - \frac{(\rho c_p)_{SWCNT}}{(\rho_f)}\right)\phi_1 + \phi_2\frac{(\rho)_{MWCNT}}{(\rho_f)}\right)\right]$$

$$\mu_{hnf} = \frac{\mu_f}{(1-\phi_1)^{2.5}(1-\phi_2)^{2.5}}$$

$$M = \frac{\sigma_f B_0^2}{b\rho_f}, \qquad Ec = \frac{u_w^2}{c_p(T_w - T_\infty)}, \qquad \beta_1 = \beta_i b,$$

$$\beta_2 = \beta_j b, E = \frac{E_0}{B_0 u_w}, P_0 = \frac{\mu_f}{K\rho_f}, Pr = \frac{v_f}{\alpha_f}, Nb = \frac{\tau D_B(C_w - C_\infty)}{v_f}, Nt = \frac{\tau D_T(T_w - T_\infty)}{T_\infty v}, Sc$$

$$= \frac{v}{D_B}, Cr = \frac{k_l}{b}, \qquad Ln = \frac{v}{D_B}, K = \frac{\eta_0 b}{v_f^2 \rho_f}, Q = \frac{Q_0}{b(\rho c_p)_f}$$

Where M is magnetic, Ec is Eckert, β_1 is thermal relaxation, β_2 is mass relaxation parameter, E is electric field factor, P_0 is porosity parameter, Pr is Prandtl, Nb is Brownian motion, Nt is thermophoresis, Sc is Schmidt, Cr is chemical reaction, Ln is Lewis term, K is couples stress term, Q is heat source or sink parameter.

Table 1
Numerical values of nanoparticles and water

Thermophysical properties Fluid phase	H₂O	Al₂O₃	CuO	Ni
$C_p\left(\frac{j}{kg}\right)k$	4179	765	385	444
$\rho(\frac{kg}{m^3})$	997.1	3970	8933	8900
$K(\frac{W}{mk})$	0.613	40	400	90.9

2.1 *Spectral Relaxation Method*

By using the SRM, the technique of Gauss-seidel relaxation is utilized in decoupling and linearizing the system of equations. The present iteration represented by $r + 1$ is utilized on the linear terms while the previous iteration represented by r is implemented on the nonlinear terms. The Chebyshev collocation approach is further employed on the iterated sequence of equations. Utilizing the SRM, the following equations were obtained:

$$f'''_{r+1} + a_{0,r}f''_{r+1} + a_{1,r} - a_{2,r}f_{r+1}^v + a_{3,r} + a_{4,r}f'_{r+1} + a_{5,r}f_{r+1} = 0 \tag{11}$$

$$b_{0,r}\theta''_{r+1} + b_{1,r}\theta'_{r+1} + b_{2,r} - b_{3,r} + b_{4,r} + b_{5,r} + QPr\theta_{r+1}$$
$$+b_{6,r}\theta'_{r+1} + b_{7,r} + b_{8,r}\theta'_{r+1} + b_{9,r}\theta''_{r+1} = 0 \tag{12}$$

$$\phi''_{r+1} + c_{0,r}\phi'_{r+1} - Cr\phi_{r+1} + c_{1,r} + c_{2,r}\phi'_{r+1} + c_{3,r}\phi''_{r+1} = 0 \tag{13}$$

subject to:

$$f_{r+1}(0,\eta) = 0, \ f'_{r+1}(0,\eta) = 1, \ \theta_{r+1}(0,\eta) = \phi_{r+1}(0,\eta) = 1 \tag{14}$$

$$f_{r+1}(\infty,\eta) = 0, \ \theta_{r+1}(\infty,\eta) = \phi_{r+1}(\infty,\eta) = 0 \tag{15}$$

The coefficients in the equation above are:

$$a_{0,r} = \frac{\mu_f \rho_{hnf}}{\mu_{hnf}\rho_f}f_r, \qquad a_{1,r} = -\frac{\mu_f \rho_{hnf}}{\mu_{hnf}\rho_f}f'^2_{r+1}, \qquad a_{2,r} = \frac{K\mu_f \rho_{hnf}}{\mu_{hnf}\rho_f}, \qquad a_{3,r} = \frac{M\mu_f \rho_{hnf}}{\mu_{hnf}\rho_f}$$

$$a_{4,r} = -\frac{M\mu_f \rho_{hnf}}{\mu_{hnf}\rho_f}, \qquad a_{5,r} = \frac{1}{K}\frac{\mu_f \rho_{hnf}}{\mu_{hnf}\rho_f}, \qquad b_{0,r} = \frac{K_{hnf}}{K_f}, \qquad b_{1,r} = \frac{Pr(\rho c_p)_{hnf}}{(\rho c_p)_f}f_{r+1}$$

$$b_{2,r} = EcPrME^2, \qquad b_{3,r} - 2EcPrMEf'_{r+1}, \qquad b_{4,r} = EcPrMf'^2_{r+1},$$
$$b_{5,r} = EcPr\frac{\mu_{hnf}}{\mu_f}f''^2_{r+1},$$

$$b_{6,r} = Nb\phi'_r, \qquad b_{7,r} = Nt(\theta'_{r+1})^2, \qquad b_{8,r} = -\beta_1 f_{r+1}f'_{r+1}, \qquad b_{9,r} = -\beta_1 f^2_{r+1}$$

$$c_{0,r} = Scf_{r+1}, \qquad c_{1,r} = \frac{Nt}{LnNb}\theta'', \qquad c_{2,r} = \beta_2 f_{r+1}f'_{r+1}, \qquad c_{3,r} = -\beta_2 f^2_{r+1}$$

A starting guess is taken to satisfies the boundary constraints Eqs. (14) and (15). The guess as used in this study are defined as follows:

$$f_0 = 1 - e^{-\eta}, \ \theta_0 = \phi_0 = e^{-\eta} \tag{16}$$

Starting from the starting guess in Eq. (16), the set of Eqs. (11)-(13) are solved iteratively. Also, discretization was further done to the iterative equations by utilizing the chebyshev collocation approach.

3. Results

The spectral relaxation method was used to solve the transformed ordinary differential Eqs. (7)-(9) along with the boundary conditions (10) numerically. Diagrams show the effect of flow parameters on velocity, concentration, and temperature profiles. It is also possible to keep track of how flow parameters affect the various engineering quantities that matter. It's depicted in Figure 2 how the chemical reaction parameter (Cr) affects velocity and concentration. The velocity and concentration profiles decrease as a result of an increase in Cr. Within the boundary layer, a chemical reaction occurs between the stress fluid and the blood-based nanofluids. Figure 2 depicts an exothermic chemical reaction, in which fluid particles lose momentum and concentration.
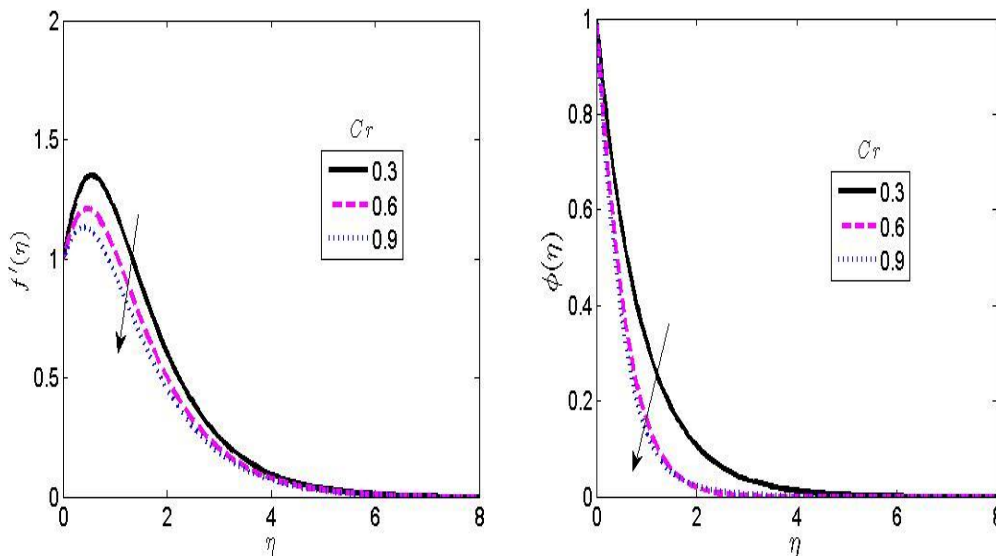

Fig. 2. Reaction of chemical reaction on the velocity and concentration plots.

Viscous dissipation (Eckert number, (Ec)) is shown in Figure 3 in relation to velocity and temperature profiles. Both the velocity and temperature profiles rise when Eckert number increases. The Eckert number is derived from the simplification of the energy equation's viscous dissipation term. Enthapyl and kinetic energy in a flow have a relationship to this. Shear forces in a fluid increase as Ec increases in value. As a result, the temperature of the fluid and the flow velocity both rise as Ec and the heat source or sink in the flow increase. Temperature and velocity profiles are shown in Figure 4 as a result of an electric field (E). The intensity of E varies experimentally depending on the size and constructive form of the cells. The propelled magnetic field was found to be susceptible to an increased value of E. Enhancement of temperature and velocity profiles can be spotted in Figure 4.
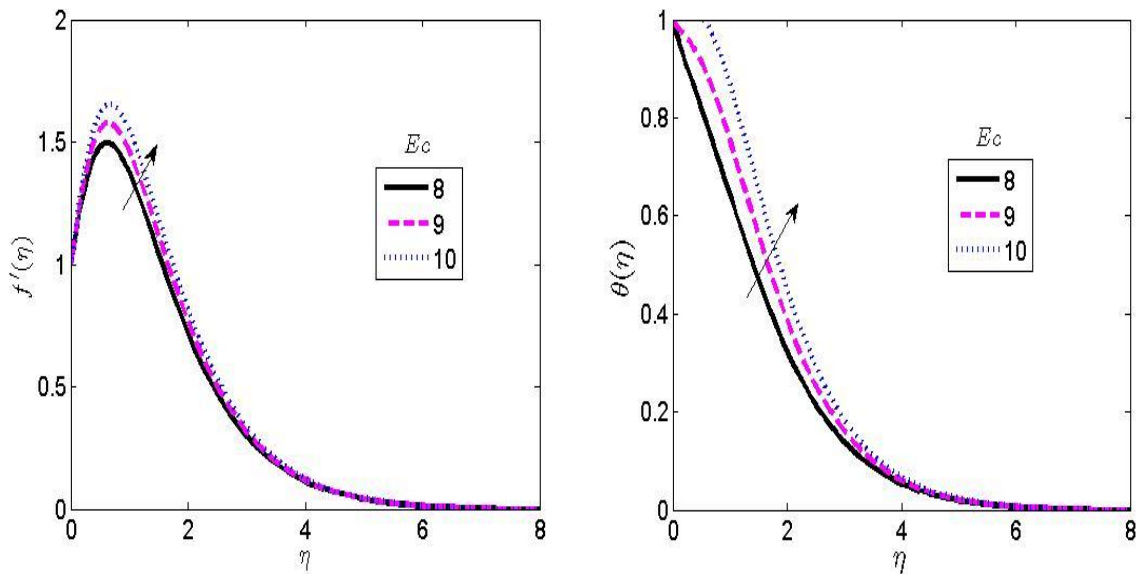

Fig. 3. Reaction of Eckert number on the velocity, temperature plots
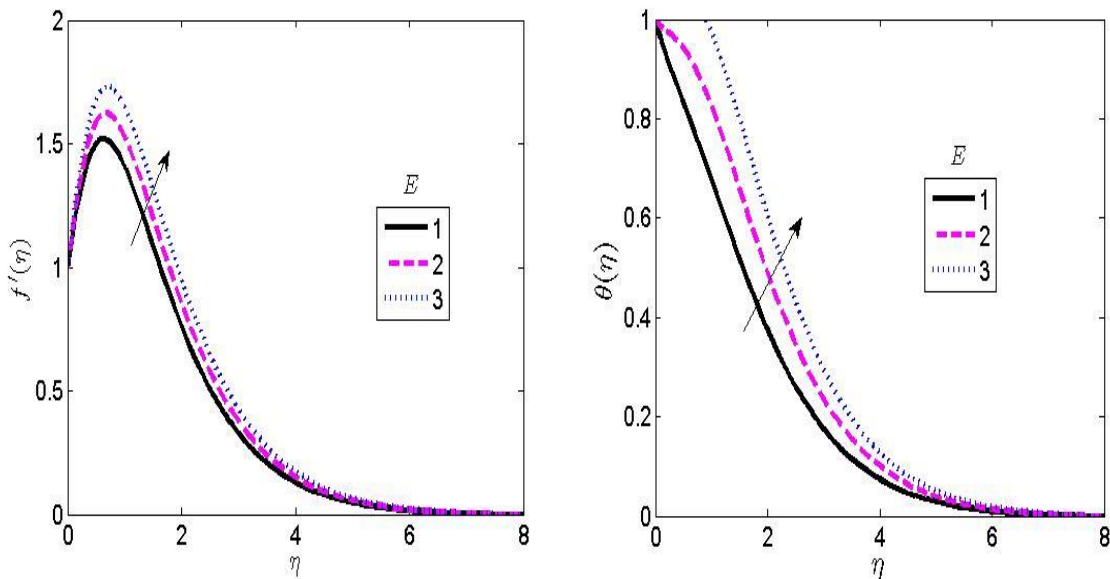

Fig. 4. Reaction of Electric field factor on the velocity, temperature plots

Magnetic field parameter (M) has an effect on the velocity profile as shown in Figure 5. To slow down the flow of an electrically conducting liquid, the Lorentz force must be introduced into the flow of the fluid. The velocity profile decreased when the magnetic parameter was in opposition to the transport phenomena. Plots of velocity and temperature as a function of Prandtl number (Pr) are shown in Figure 6. According to Prandtl, there is a connection between kinematic viscosity and thermal conductivity. Within the boundary layer, it depicts the ratio of momentum diffusion to thermal diffusion. Depreciation of the momentum and thermal boundary layer thickness is observed when Pr is large. A thermal radiation parameter's effect on velocity and temperature profiles can be seen in Figure 7. The convective flow is said to be aided by thermal radiation. The viscosity of blood-based nanofluids decreases as a result of the boundary layer becoming hotter as a result of increased thermal radiation. As a result, the momentum and thermal boundary layer are enhanced when the thermal radiation is higher.
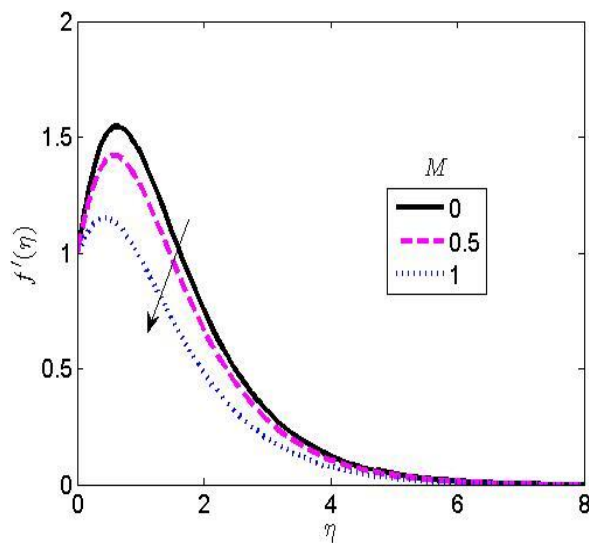

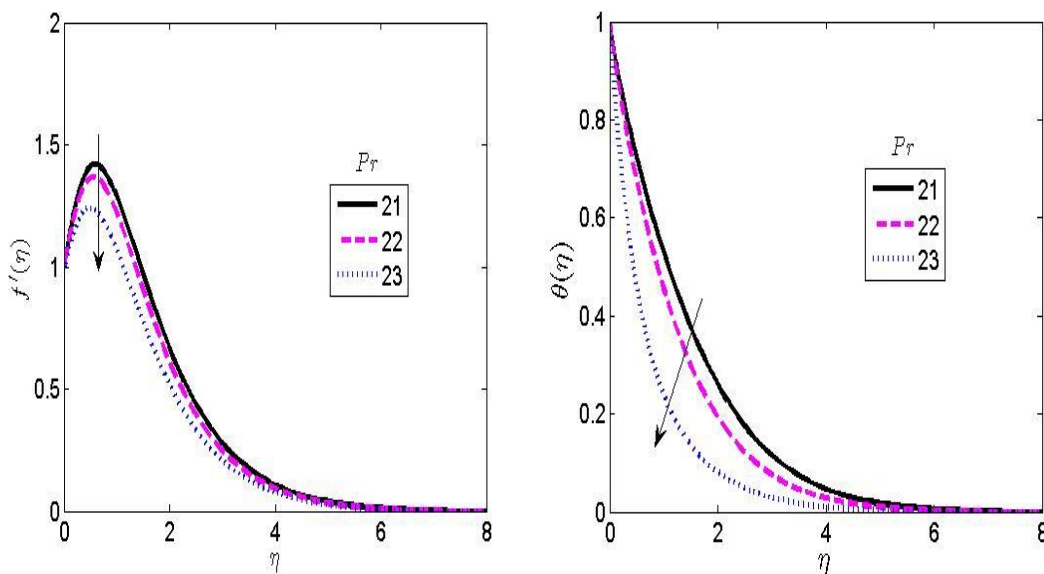**Fig. 5.** Reaction of Magnetic on the velocity profile

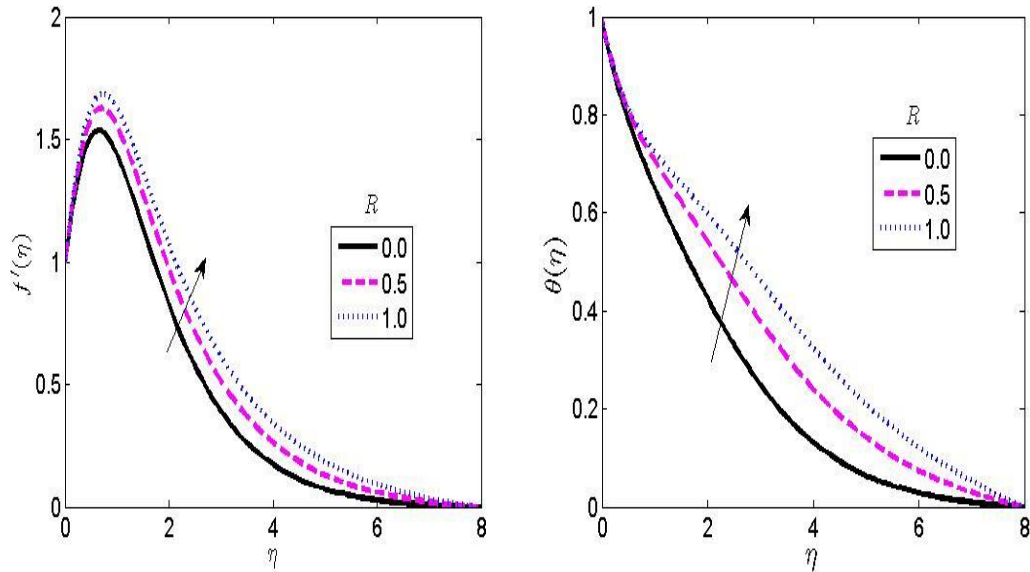**Fig. 6.** Reaction of Prandtl on the velocity, temperature plots

Fig. 7. Reaction of Thermal radiation on the velocity, temperature plots

Velocity and concentration profiles can be seen in Figure 8 as a result of Schmidt number (Sc). Kinetic viscosity and mass diffusivity of the fluid are both referred to as "Sc" in this context. When the kinematic viscosity exceeds the mass diffusivity, this indicates a high Schmidt number. To put it another way, when Sc is increased, the buoyancy effects of concentration will have a negative impact on the rate of mass transfer and the concentration profile. Figure 9 depicts the velocity profile as a function of the Couple stress parameter (K). Figure 9 shows an increase in the velocity of the fluid and the thickness of the hydrodynamic boundary layer as a result of an increasing K value. Physically, the fluid flow was propelled by the wall's temperature, which increased the flow's velocity. The fluids within the layers move more quickly as a result of an increase in K. The effect of heat generation or sink on temperature and velocity profiles can be seen in Figure 10. The velocities and temperatures rise as a result of an increase in heat generation (Q). Collision between particles causes a temperature increase in the boundary layer as the fluid moves. The collision generates more energy and, as a result, expands the hydrodynamic boundary layer.
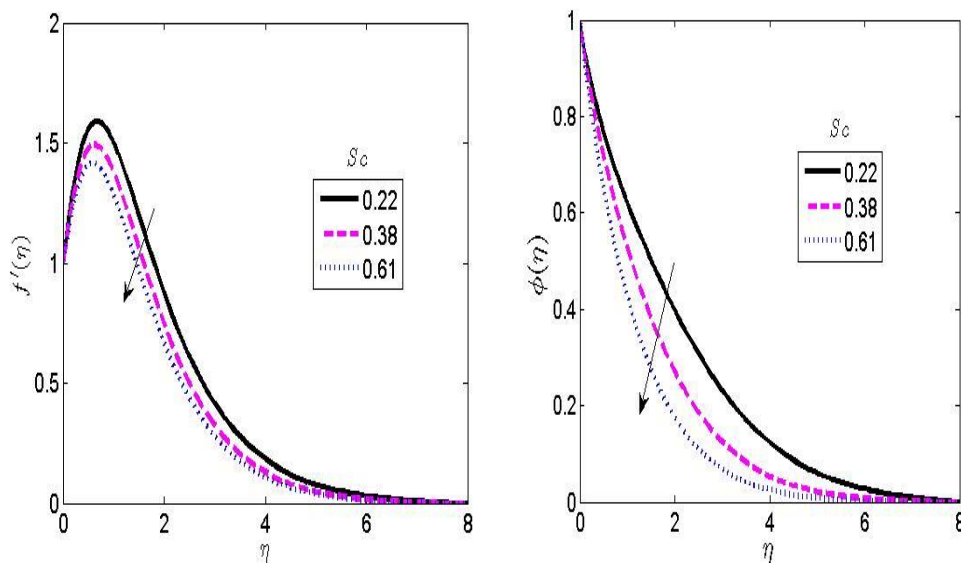

Fig. 8. Reaction of Schmidt number on the velocity, concentration plots
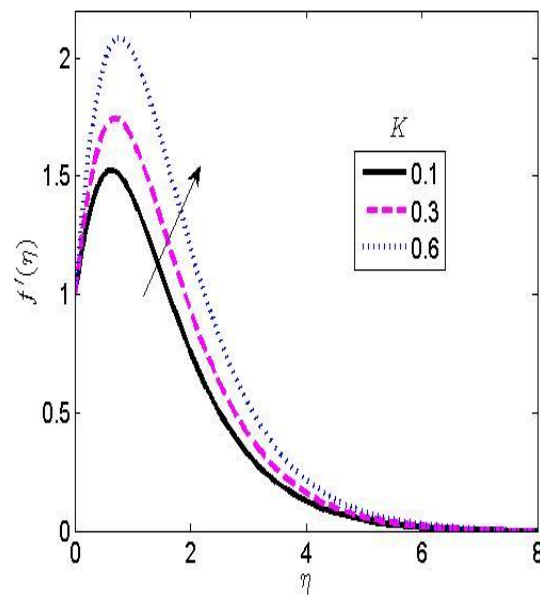
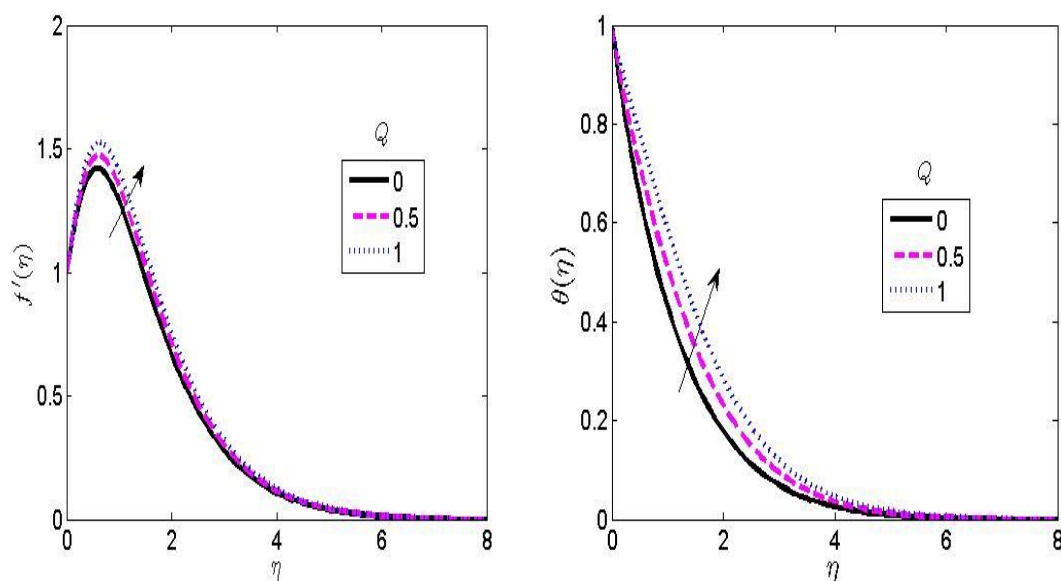**Fig. 9.** Reaction of Couple stress term on velocity plot

Fig. 10. Reaction of heat generation on the velocity and temperature plots

4. Conclusions

This paper researched the electro-hydrodynamics of blood-based nanofluids flow with the theories of Cattaneo-Christov model. Heat generation and thermal radiation are considered with first order chemical reaction. The model analysis were answered numerically utilizing spectral relaxation techniques. From the outcomes:

    i.   Higher electric field factor is noticed to enhance both velocity and temperature profile;

    ii.   Increase in Eckert number is observed to increase both thermal and hydrodynamic boundary layer thickness;

iii.   A higher value of K extetends the hole and allows for higher fluid flow by increasing the fluid velocity;

iv.   Increase in Pr depreciates both velocity and temperature profile; and

v.   A higher value of Sc depreciates the skin friction and Sherwood number.

References

[1]   Waqas, Hassan, Metib Alghamdi, Taseer Muhammad, and Muhammad Altaf Khan. "Bioconvection transport of magnetized Walter's B nanofluid across a cylindrical disk with nonlinear radiative heat transfer." *Case Studies in Thermal Engineering* 26 (2021): 101097. https://doi.org/10.1016/j.csite.2021.101097

[2]   Bibi, Aneela, and Hang Xu. "Peristaltic channel flow and heat transfer of Carreau magneto hybrid nanofluid in the presence of homogeneous/heterogeneous reactions." Scientific Reports 10, no. 1 (2020): 1-20. https://doi.org/10.1038/s41598-020-68409-0

[3]   Shaheen, Naila, Muhammad Ramzan, Ahmed Alshehri, Zahir Shah, and Poom Kumam. "Soret–Dufour impact on a three-dimensional Casson nanofluid flow with dust particles and variable characteristics in a permeable media." *Scientific Reports* 11, no. 1 (2021): 1-21. https://doi.org/10.1038/s41598-021-93797-2

[4]   Zubair, Muhammad, Muhammad Jawad, Ebenezer Bonyah, and Rashid Jan. "MHD Analysis of Couple Stress Hybrid Nanofluid Free Stream over a Spinning Darcy-Forchheimer Porous Disc under the Effect of Thermal Radiation." *Journal of Applied Mathematics* 2021 (2021). https://doi.org/10.1155/2021/2522155

[5]   Sadiq, Kashif, Fahd Jarad, Imran Siddique, and Bagh Ali. "Soret and radiation effects on mixture of ethylene glycol-water (50%-50%) based Maxwell nanofluid flow in an upright channel." *Complexity* 2021 (2021). https://doi.org/10.1155/2021/5927070

[6]   Upadhay, Mamatha S., and C. S. K. Raju. "Cattaneo-Christov on heat and mass transfer of unsteady Eyring Powell dusty nanofluid over sheet with heat and mass flux conditions." *Informatics in Medicine unlocked* 9 (2017): 76-85. https://doi.org/10.1016/j.imu.2017.06.001

[7]   Rashidi, M. M., M. T. Akolade, M. M. Awad, A. O. Ajibade, and I. Rashidi. "Second law analysis of magnetized Casson nanofluid flow in squeezing geometry with porous medium and thermophysical influence." *Journal of Taibah University for Science* 15, no. 1 (2021): 1013-1026. https://doi.org/10.1080/16583655.2021.2014691

[8]   Vijaya, Kolli, and Gurrampati Venkata Ramana Reddy. "Magnetohydrodynamic casson fluid flow over a vertical porous plate in the presence of radiation, soret and chemical reaction effects." *Journal of Nanofluids* 8, no. 6 (2019): 1240-1248. https://doi.org/10.1166/jon.2019.1684

[9]   Suneetha, K., S. M. Ibrahim, and GV Ramana Reddy. "Radiation and heat source effects on MHD flow over a permeable stretching sheet through porous stratum with chemical reaction." *Multidiscipline Modeling in Materials and Structures* (2018). https://doi.org/10.1108/MMMS-12-2017-0159

[10]   Reddy, G. V. R., and Y. Hari Krishna. "Soret and dufour effects on MHD micropolar fluid flow over a linearly stretching sheet, through a non-darcy porous medium." *International Journal of Applied Mechanics and Engineering* 23, no. 2 (2018). https://doi.org/10.2478/ijame-2018-0028

[11]   Nagasantoshi, P., G. V. Reddy, M. Gnaneswara Reddy, and P. Padma. "Heat and mass transfer of Non-Newtonian Nanofluid flow over a stretching sheet with non-uniform heat source and Variable viscosity." *Journal of Nanofluids* 7, no. 5 (2018): 821-832. https://doi.org/10.1166/jon.2018.1517

[12]   Lakshmi, R., K. R. Jayarami, K. Ramakrishna, and GV RAMANA Reddy. "Numerical Solution of MHD flow over a moving vertical porous plate with heat and Mass Transfer." *Int. J. Chem. sci 12 (14), 1487* 1499 (2014).

[13]   Mabood, F., A. Shafiq, T. Hayat, and S. Abelman. "Radiation effects on stagnation point flow with melting heat transfer and second order slip." *Results in Physics* 7 (2017): 31-42. https://doi.org/10.1016/j.rinp.2016.11.051

[14]   Hayat, Tasawar, Sumaira Qayyum, Maria Imtiaz, and Ahmed Alsaedi. "Radiative flow due to stretchable rotating disk with variable thickness." *Results in Physics* 7 (2017): 156-165. https://doi.org/10.1016/j.rinp.2016.12.010

[15]   Nayak, M. K., S. Shaw, Hassan Waqas, O. D. Makinde, Metib Alghamdi, and Taseer Muhammad. "Comparative study for magnetized flow of nanofluids between two parallel permeable stretching/shrinking surfaces." *Case Studies in Thermal Engineering* 28 (2021): 101353. https://doi.org/10.1016/j.csite.2021.101353

[16]   Shah, Zahir, Abdullah Dawar, I. Khan, Saeed Islam, Dennis Ling Chaun Ching, and Aurang Zeb Khan. "Cattaneo-Christov model for electrical magnetite micropoler Casson ferrofluid over a stretching/shrinking sheet using effective thermal conductivity model." *Case Studies in Thermal Engineering* 13 (2019): 100352. https://doi.org/10.1016/j.csite.2018.11.003

[17]   Abo-zaid, Omima A., R. A. Mohamed, F. M. Hady, and A. Mahdy. "MHD Powell–Eyring dusty nanofluid flow due to stretching surface with heat flux boundary condition." *Journal of the Egyptian Mathematical Society* 29, no. 1 (2021): 1-14. https://doi.org/10.1186/s42787-021-00123-w